A strategy for the identification of protein architectures directly from ion mobility mass spectrometry data reveals stabilizing subunit interactions in light harvesting complexes

Margit Kaldmäe, Cagla Sahin, Mihkel Saluri, Erik G. Marklund, and Michael Landreh

Table S1. Masses for PE and PC complexes and dissociation products. Standard deviations indicate the mass error between charge states. Predicted masses are based on the experimentally determined masses for α- and β-subunits.

Complex	Measured Mass (Da)	Standard Deviation (Da)	Predicted Mass (Da)
PE			
α	18 861	1.2	
β	20 186	1.2	
γ'	27 - 28 kDa		
γ''	31 – 32 kDa		
$\alpha_6\beta_6\gamma$'	262 279	65	
$\alpha_6\beta_6\gamma$''	265 964	108	
$\alpha_6\beta_5\gamma$'	241749	92	242 093
$\alpha_6\beta_5\gamma$''	244 654	50	245 778
$\alpha_5\beta_6\gamma$'	242 886	50	243 418
$\alpha_5\beta_6\gamma$''	246 004	45	245 778
$\alpha_6\beta_4\gamma$'	221 059	88	221 907
$\alpha_4\beta_6\gamma$' / $\alpha_6\beta_4\gamma$''	223 716	44	224 557 / 225 592
$\alpha_4\beta_6\gamma$''	226 791	89	228 242
$\alpha_5\beta_5\gamma$'	222 418	113	223 232
$\alpha_5\beta_5\gamma$''	225 553	51	226 917
PC			
α	18 151	1.2	
β	19 240	1.0	
γ	33 -34 kDa		
$\alpha\beta$	37526	52	37 391
$\alpha_3\beta_3$	112 456	48	112 173
$\alpha_6\beta_6$	225 280	79	224 346
$\alpha_6\beta_6\gamma$	259 135	159	
$\alpha_5\beta_6$	206 901	65	206 195
APC			
α	17 938	5.2	
β	17 817	2.6	
$\alpha_3\beta_3$	109 495	91	107 265
$\alpha_2\beta_3$	89 888	11	89 448
$\alpha_2\beta_2$	71 913	86	71 510

Table S2. CCS values for PE and PC complexes.

Complex

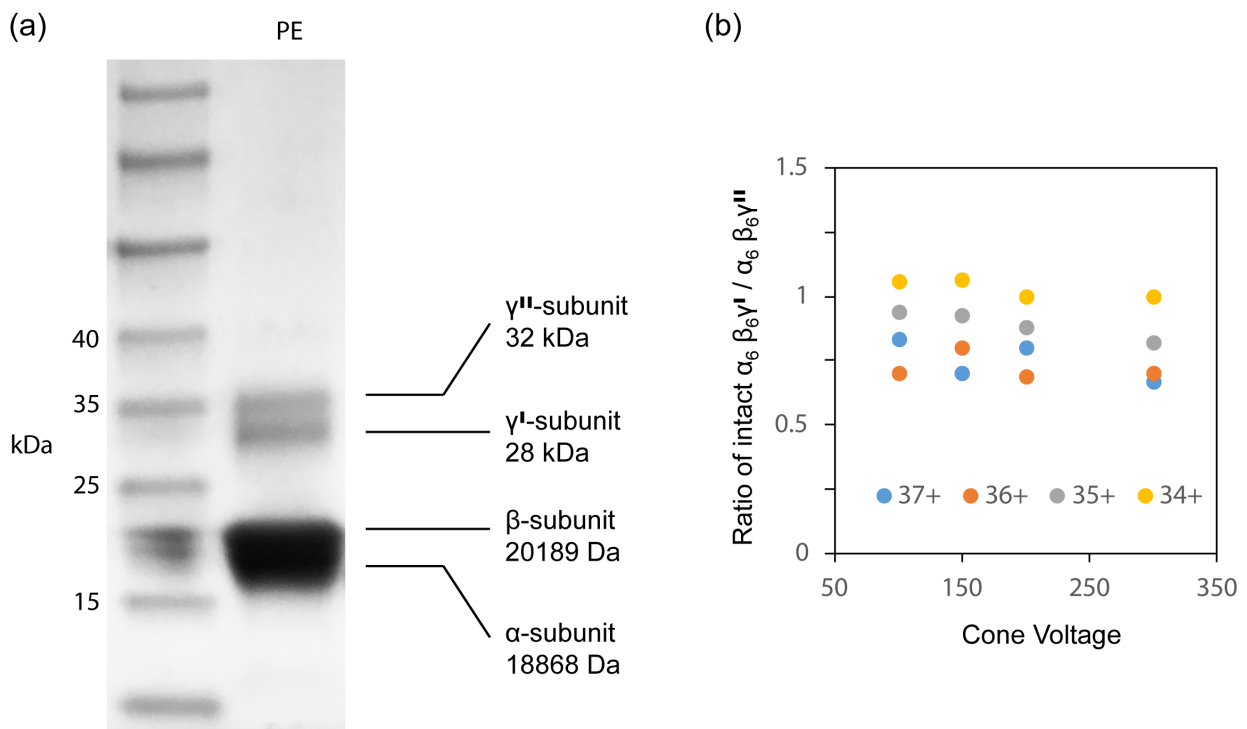| $\alpha_6\beta_6\gamma$' PE	Charge state	CCS (Ä^2)
	35	11 353
	36	11 299
	37	11 289
	38	11 301
$\alpha_6\beta_6\gamma$'' PE		
	35	11 476
	36	11 462
	37	11 418
	38	11 433
$\alpha_6\beta_6\gamma$ PC		
	35	11 298
	36	11 368
	37	11 382
	38	11 393
$\alpha_6\beta_6$ PC		
	34	10 047
	35	10 363
	36	10 491
	37	10 619

Figure S1. (a) SDS-PAGE analysis of PE shows the presence of two linker proteins (γ' and γ") which differ by less than 5 kDa. The indicated masses were calculated from the intact PE complexes (Table S1). **(b)** Comparison of the ratio of intact $\alpha_6\beta_6\gamma'$ and $\alpha_6\beta_6\gamma"$ PE for each charge state at each cone voltage shows similar gas-phase stabilities for both complexes.
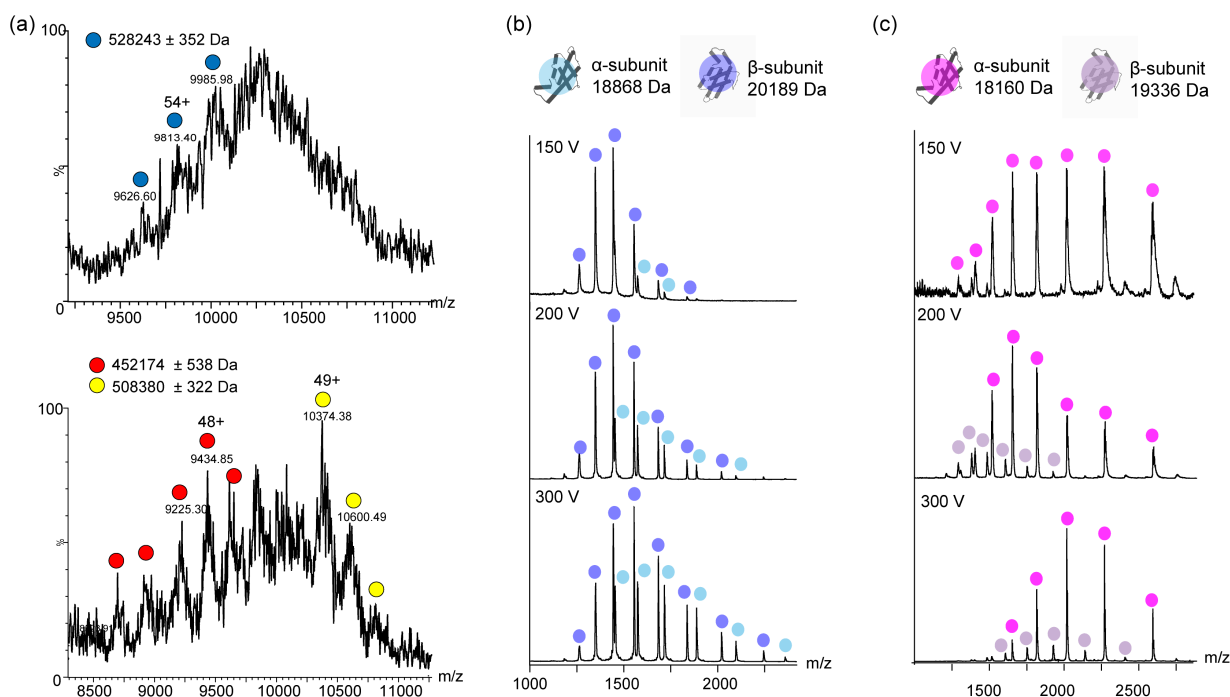
Figure S2. PE and PC complexes form dimers and release different subunits. **(a)** Top: The enlarged high *m/z* region of the spectrum in Fig. 1a shows peaks indicating complexes of approximately 530 kDa in size (blue dots). Bottom: Zoom in the high *m/z* region of the spectrum in Fig. 1b reveals the presence of two distinct dimeric PC complexes corresponding in mass to two $\alpha_6\beta_6$ (red dots) or two $\alpha_6\beta_6\gamma$ complexes (yellow dots). **(b)** Zoom of the low *m/z* region of the spectra in Fig. 1a indicates sequential release of β- and then α-subunits (bright and dark pink, respectively). **(c)** Zoom of the low *m/z* region of the spectra in Fig. 1b shows predominant release of α-subunits over β-subunits (bright and dark blue, respectively) in response to collisional dissociation.
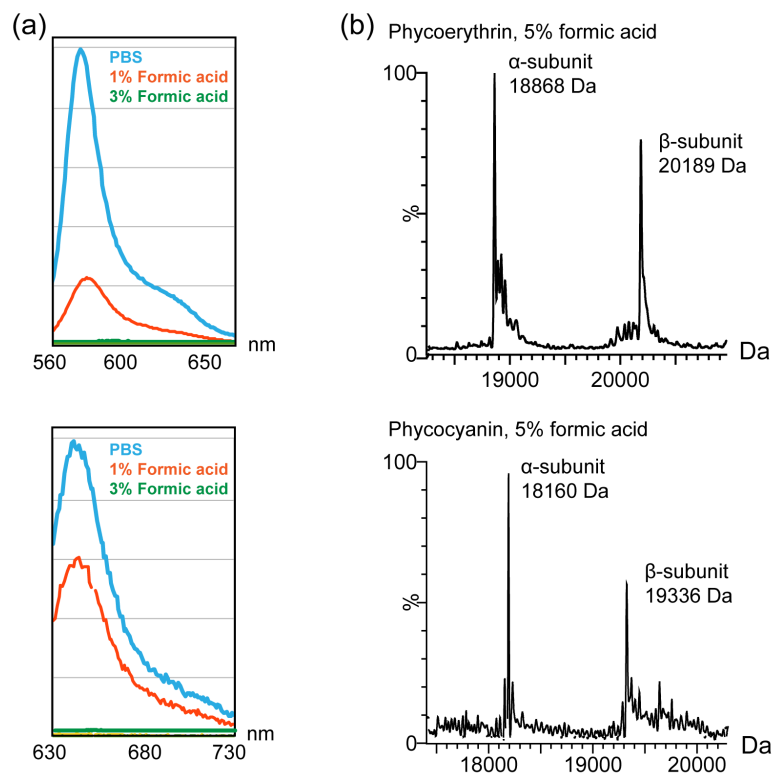
Figure S3. (a) Fluorescence spectroscopy was used to monitor acid-induced dissociation of PE and PC. **(b)** MS spectra of the completely dissociated complexes show that α- and β-subunits of PE and PC give similar MS responses.
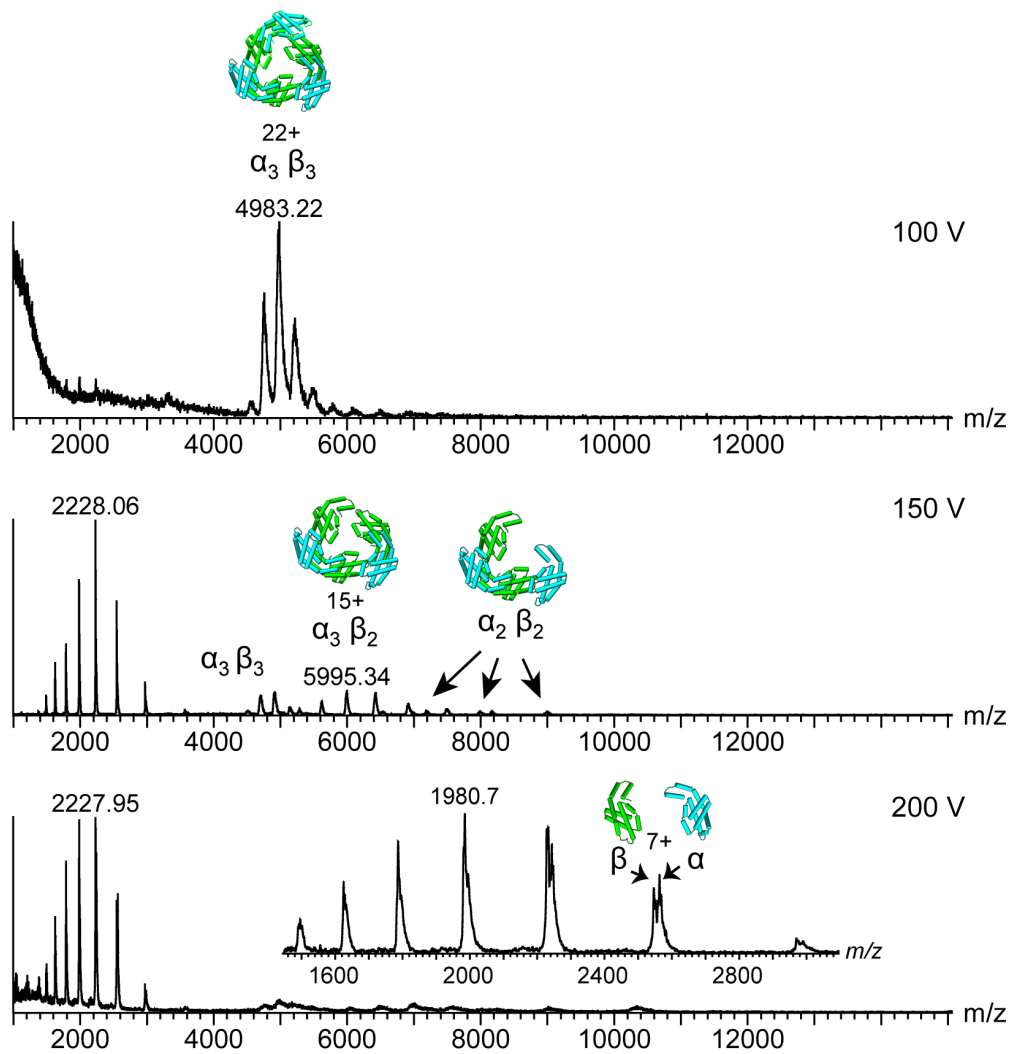
Figure S4. Intact mass analysis and gas-phase dissociation of APC. Using gentle ionization conditions, a homogeneous population of intact APC hetero-hexamers with no additional components can be detected. Raising the cone voltage to induce gas-phase dissociation releases individual α- and β-subunits (insert).
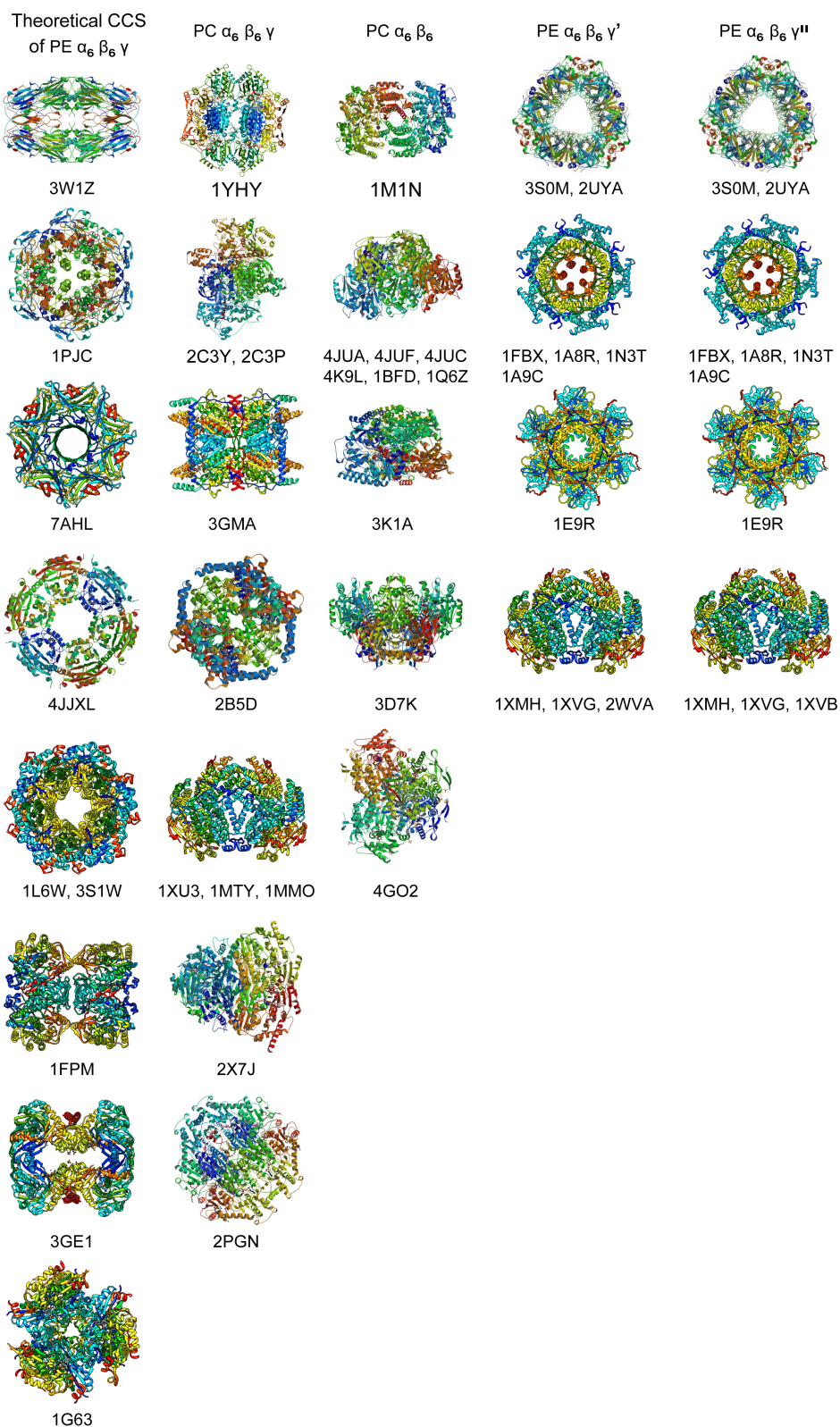
Figure S5. Top ten structural neighbours of the different PE and PC complexes identified by the PDB search. First column, matches for the theoretical CCS and MW of $\alpha_6\beta_6\gamma$ PE. Second column, matches for the experimental CCS and MW of $\alpha_6\beta_6\gamma$ PC. Third column, matches for $\alpha_6\beta_6$ PC. Fourth and fifth column, matches for $\alpha_6\beta_6\gamma'$ and $\alpha_6\beta_6\gamma''$ PE.